Phase diagrams of spin-2 Floquet spinor Bose-Einstein condensates

Yan-Ling Pan,[1] Qi Li,[1] Gong-Ping Zheng,[1, 2, *] and Yongping Zhang[1, 2, 3, †]

[1] *College of Physics and Electronic Information Engineering, Qinghai Normal University, Xining, Qinghai 810016, China*

[2] *Academy of Plateau Science and Sustainability, Xining, Qinghai 810016, China*

[3] *Institute for Quantum Science and Technology, Department of Physics, Shanghai University, Shanghai 200444, China*

We propose the realization of a spin-2 Floquet spinor Bose-Einstein condensate via Floquet engineering of the quadratic Zeeman energy. In the Floquet system, the coupling strengths of all angular-momentum-conserving spin-flip processes are renormalized by driving-parameter-dependent Bessel functions. Such Floquet-engineered interactions significantly enriches possible ground states in homogeneous gases. The resulting phase diagrams, which map the distributions of these possible ground states, are presented in the space of the driving parameters.

I. INTRODUCTION

Soon after the initial experimental realizations of an atomic scale Bose-Einstein condensate (BEC), spinor BECs immediately attracted significant experimental and theoretical interest due to their richer degrees of freedom compared to scalar ones [1, 2]. They provide fundamental platforms for studying interacting many-body physics with spin. A spin-1 spinor BEC features not only a density-density interaction but also a distinct spin-dependent interaction, The ground-state phase including polar and ferromagnetic is determined by the sign of the latter [3, 4]. The presence of an external magnetic field can introduce a broken-axisymmetry phase in spin-1 BECs with ferromagnetic interactions (i.e., with a negative spin-dependent interaction sign) [5]. The ground states, spin structures and dynamics have been experimentally studied in various spin-1 BEC systems [6–8]. In experiments, the quadratic Zeeman energy can be tuned via a microwave-frequency magnetic field [9, 10]. Quantum quenches of this parameter can trigger quantum phase transitions, leading to rich non-equilibrium phenomena [11–13]. Furthermore, merging two distinct spin-1 spinor BECs to form a quantum mixture has been shown to yield a complex and physically meaningful phase diagram [14–17]. Extending the system to the spin-2 spinor BEC reveals even greater complexity, as it possesses two distinct spin-dependent interactions [18–20]. This results in phase diagrams that include, in addition to polar and ferromagnetic phases, a cyclic phase [21–26]. The spin-2 system is also a promising platform for generating quantum entanglement [27, 28] and studying topological order parameters [29, 30]. The study of mixtures combining spin-2 and spin-1 spinors is also highly interesting [31, 32].

The fundamental physics of spinor BECs is largely governed by spin-dependent interactions. However, the experimental tuning of these interaction strengths remains a challenge [33]. In a notable recent study, Fujimoto and Uchino proposed a method to achieve such tunability via Floquet engineering of the quadratic Zeeman energy in a spin-1 spinor BEC [38]. In a spin-1 system, the spin-dependent interactions include a spin-flip process, $2|0\rangle \leftrightarrow |-1\rangle + |1\rangle$, as only this process conserves angular momentum. This process has attracted significant research interest [7, 19, 34–37]. It is noteworthy that in their proposed Floquet-engineered system, the high-frequency modulation of the quadratic Zeeman energy specifically modifies the coupling strength of this particular spin-flip process. This modification leads to substantial changes in the possible ground states and phase diagram for ferromagnetic spin-dependent interactions [38]. More recently, this Floquet engineering approach has been applied to study stripe supersolid phases in spin-1 spinor BECs with experimentally realizable spin-orbit coupling [39].

In this work, we apply the Floquet engineering of the quadratic Zeeman energy to a spin-2 spinor BEC. Owing to the greater number of spin degrees of freedom, two distinct spin-dependent interactions in spin-2 condensates possess multiple spin-flip processes that conserve angular momentum [2]. Within the high-frequency approximation for the periodically driven quadratic Zeeman energy, we find that the coupling strengths of all these spin-flip processes are modulated by Bessel functions of the first kind. Notably, different processes are governed by different Bessel functions, depending on the specific driving parameters. Consequently, Floquet engineering not only tunes the strengths of these spin-flip interactions but also alters their relative magnitudes. Given the fundamental role of these interactions, this Floquet engineering approach provides a powerful means for the quantum manipulation of spin-2 condensates. To illustrate the difference with a conventional spin-2 condensate, we demonstrate that the resulting Floquet system can be interpreted as possessing the same basic interactions as a conventional one, but with two additional, effective spin-flip interactions derived from the original two spin-dependent interactions.

The introduction of these two Floquet-engineered interactions significantly enriches possible ground states in homogeneous spin-2 Floquet spinor Bose-Einstein con-

* Corresponding author: zhenggongping@aliyun.com
† Corresponding author: yongping11@t.shu.edu.cn

densates (BECs). The three fundamental ground-state phases-polar, ferromagnetic, and cyclic-now exhibit numerous variants. The Bessel-function modulations can alter the energies of the ground states or directly participate in the construction of the spinor wavefunctions. Notably, we identify novel ground states that are absent in conventional spinor BECs. Finally, we map the distribution of these possible ground states into a phase diagram for specific interaction parameters highly relevant to ^{87}Rb spinor BECs [19].

The remainder of the paper is organized as follows. In Sec. II, we present the model for a spin-2 spinor BEC with a modulated quadratic Zeeman energy. Using the high-frequency approximation, we derive an effective Hamiltonian to describe the resulting Floquet system. In Sec. III, we identify possible ground states of the spin-2 Floquet spinor BEC, including the polar, ferromagnetic, and cyclic phases. In Sec. IV, corresponding phase diagrams are presented in the parameter space of the driving field. A summary of our findings is provided in Sec. V. Finally, the Appendix presents an alternative derivation of a similar effective Hamiltonian using the high-frequency expansion method.

II. SPIN-2 FLOQUET SPINOR BOSE CONDENSATES

The spin-2 spinor BEC features a vector field operator $\hat{\psi} = \left(\hat{\psi}_2, \hat{\psi}_1, \hat{\psi}_0, \hat{\psi}_{-1}, \hat{\psi}_{-2}\right)^T$, with $\hat{\psi}_{m_F}$ representing the wave function of the Zeeman states $|F=2, m_F\rangle \equiv |m_F\rangle$ ($m_F = \{2, 1, 0, -1, -2\}$) within a spin $F=2$ manifold. The BEC system is described by the Hamiltonian [2],

$$\begin{aligned}\hat{H} &= \int d\mathbf{r}\hat{\psi}^\dagger \left(-\frac{\hbar^2\nabla^2}{2M}\right)\hat{\psi} + \int d\mathbf{r}\hat{\psi}^\dagger \left(qF_z^2\right)\hat{\psi} \\ &+ \frac{c_0}{2}\int d\mathbf{r}\left(\hat{\psi}^\dagger\hat{\psi}\right)^2 + \frac{c_1}{2}\int d\mathbf{r}\left(\hat{\psi}^\dagger\mathbf{F}\hat{\psi}\right)\cdot\left(\hat{\psi}^\dagger\mathbf{F}\hat{\psi}\right) \\ &+ \frac{c_2}{2}\int d\mathbf{r}\left(\hat{\psi}^T A\hat{\psi}\right)^\dagger\left(\hat{\psi}^T A\hat{\psi}\right). \end{aligned} \tag{1}$$

Here, the first term represents the kinetic energy, where M is the atomic mass. $\mathbf{F} = (F_x, F_y, F_z)$ denotes the spin-2 Pauli matrices [2]. The second term is the effective quadratic Zeeman energy, with q being its magnitude. The remaining three terms describe the interactions: c_0 is the spin-independent interaction coefficient, representing the density-density interaction; c_1 and c_2 are spin-dependent interaction coefficients describing the spin-spin interaction and interaction through the spin-singlet scattering channel respectively. A is associated with the amplitude of the spin-singlet pair [21],

$$A = \begin{pmatrix} 0 & 0 & 0 & 0 & 1 \\ 0 & 0 & 0 & -1 & 0 \\ 0 & 0 & 1 & 0 & 0 \\ 0 & -1 & 0 & 0 & 0 \\ 1 & 0 & 0 & 0 & 0 \end{pmatrix}, \tag{2}$$

which is an antisymmetric matrix. The field operator of the spin-singlet state becomes $\hat{\psi}^T A\hat{\psi}$.

In experiments, the quadratic Zeeman shift is tunable [9–13]. It can be experimentally adjusted by applying a linearly polarized microwave-frequency magnetic field which off-resonantly induces the transition between the $|F=2, m_F=0\rangle$ and $|F=1, m_F=0\rangle$ hyperfine states. The transition, which has the coupling strength Ω, is detuned by δ. The quadratic Zeeman shift $q \propto \hbar\Omega^2/\delta$ [10]. By periodically modulating the strength Ω (from the modulation of the magnitude of the magnetic field), we implement the quadratic Zeeman shift as [38]

$$q = q_0 + Q\cos(\omega t), \tag{3}$$

where ω and Q are the driving frequency and amplitude, respectively, and q_0 is the averaged oscillation value. We assume the modulation is high-frequency, i.e., the driving frequency is much larger than other typical energy scales of the system.

Under the high-frequency assumption, the spinor system can be described in a time-independent way. This can be carried out by performing a unitary transformation to cancel the time dependence $Q\cos(\omega t)$ and by averaging the resulting Hamiltonian over oscillating periods [40]. The time-dependent unitary transformation is $\hat{\psi} = U\hat{\phi}$ with the new field operator $\hat{\phi} = \left(\hat{\phi}_2, \hat{\phi}_1, \hat{\phi}_0, \hat{\phi}_{-1}, \hat{\phi}_{-2}\right)^T$, and $U = \exp\left(-i\mathcal{Q}\sin(\omega t)F_z^2\right)$ with

$$\mathcal{Q} = Q/(\hbar\omega). \tag{4}$$

Substituting the transformation into $\hat{H} - i\hbar\int d\mathbf{r}\hat{\psi}^\dagger\partial\hat{\psi}/\partial t$, we obtain

$$\begin{aligned}\hat{H}' &= \int d\mathbf{r}\hat{\phi}^\dagger\left(-\frac{\hbar^2\nabla^2}{2M}\right)\hat{\phi} + \int d\mathbf{r}\hat{\phi}^\dagger\left(q_0F_z^2\right)\hat{\phi} \\ &+ \frac{c_0}{2}\int d\mathbf{r}\left(\hat{\phi}^\dagger\hat{\phi}\right)^2 + H'_{\rm sd}(t,\hat{\phi}). \end{aligned} \tag{5}$$

The resulting spin-dependent interactions $H'_{\rm sd}(t,\hat{\phi})$ become very complicate and time-dependent in the way of the presence of factors $\exp[\pm ij\mathcal{Q}\sin(\omega t)]$ (with j an integer) in the front of coupling strengths in all spin-flip processes. Nevertheless, $H'_{\rm sd}(t,\hat{\phi})$ can be greatly simplified after performing the time average. Physically, the unitary transformation may be considered as displacing the system into the fast oscillating frame of the quadratic Zeeman shift. In this frame, the system is stationary. This can be achieved by performing the time average to $\hat{H}'$, i.e., $\hat{H}_{\rm eff} = \omega/(2\pi)\int_0^{2\pi/\omega} dt\hat{H}'$ [40], Finally, we obtain the effective Hamiltonian,

$$\begin{aligned}\hat{H}_{\rm eff} &= \int d\mathbf{r}\hat{\phi}^\dagger\left(-\frac{\hbar^2\nabla^2}{2M}\right)\hat{\phi} + \int d\mathbf{r}\hat{\phi}^\dagger\left(q_0F_z^2\right)\hat{\phi} \\ &+ \frac{c_0}{2}\int d\mathbf{r}\left(\hat{\phi}^\dagger\hat{\phi}\right)^2 + \frac{c_1}{2}\int d\mathbf{r}\left(\hat{\phi}^\dagger\mathbf{F}\hat{\phi}\right)\cdot\left(\hat{\phi}^\dagger\mathbf{F}\hat{\phi}\right) \\ &+ \frac{c_2}{2}\int d\mathbf{r}\left(\hat{\phi}^T A\hat{\phi}\right)^\dagger\left(\hat{\phi}^T A\hat{\phi}\right) + \hat{H}_{\rm sf}. \end{aligned} \tag{6}$$

In comparison with the original Hamiltonian $\hat{H}$, the Floquet system $\hat{H}_{\text{eff}}$ possesses additional Floquet engineered spin-flip couplings $\hat{H}_{\text{sf}}$,

$$\begin{aligned}\hat{H}_{\text{sf}} =& \frac{c_1}{2}\int d\mathbf{r}\left\{\left[J_0(2\mathcal{Q})-1\right]\left(6\hat{\phi}_0^\dagger\hat{\phi}_0^\dagger\hat{\phi}_1\hat{\phi}_{-1}+2\sqrt{6}\hat{\phi}_1^\dagger\hat{\phi}_1^\dagger\hat{\phi}_2\hat{\phi}_0+2\sqrt{6}\hat{\phi}_{-1}^\dagger\hat{\phi}_{-1}^\dagger\hat{\phi}_0\hat{\phi}_{-2}\right)+4\left[J_0(6\mathcal{Q})-1\right]\hat{\phi}_{-1}^\dagger\hat{\phi}_1^\dagger\hat{\phi}_2\hat{\phi}_{-2}\right.\\ &\left.+2\sqrt{6}\left[J_0(4\mathcal{Q})-1\right]\left(\hat{\phi}_{-1}^\dagger\hat{\phi}_0^\dagger\hat{\phi}_1\hat{\phi}_{-2}+\hat{\psi}_0^\dagger\hat{\psi}_1^\dagger\hat{\phi}_2\hat{\phi}_{-1}\right)+\text{H.c.}\right\}+\frac{c_2}{2}\int d\mathbf{r}\left\{2\left[J_0(8\mathcal{Q})-1\right]\hat{\phi}_0^\dagger\hat{\phi}_0^\dagger\hat{\phi}_2\hat{\phi}_{-2}\right.\\ &\left.-4\left[J_0(6\mathcal{Q})-1\right]\hat{\phi}_{-1}^\dagger\hat{\phi}_1^\dagger\hat{\phi}_2\hat{\phi}_{-2}-2\left[J_0(2\mathcal{Q})-1\right]\hat{\phi}_0^\dagger\hat{\phi}_0^\dagger\hat{\phi}_1\hat{\phi}_{-1}+\text{H.c.}\right\}.\end{aligned} \tag{7}$$

During deriving the effective Hamiltonian, we already use $\exp[\pm ij\mathcal{Q}\sin(\omega t)]=\sum_n J_n(j\mathcal{Q})\exp(\pm in\omega t)$ with J_n the n-th order Bessel function of the first kind. Only J_0 (i.e.,n=0) are retained in $\hat{H}_{\text{sf}}$ due to the time average.

Following the convention by Fujimoto and Uchino [38], we name the Floquet engineered $\hat{H}_{\text{eff}}$ as spin-2 Floquet spinor BECs. In spin-1 systems, the difference between conventional and Floquet spinor BECs lies in that the Floquet one has an extra spin-exchange process of $2|0\rangle \leftrightarrow |-1\rangle+|1\rangle$, which is the only spin-flip coupling conserving angular momentum [38, 39]. Similarly, the spin-2 Floquet spinor BEC possesses extra spin-flip interacting couplings represented by $\hat{H}_{\text{sf}}$. For a spin-2 spinor BEC, the spin-spin interaction, $(\hat{\psi}^\dagger\mathbf{F}\hat{\psi})\cdot(\hat{\psi}^\dagger\mathbf{F}\hat{\psi})$, is composed of density couplings such as $\hat{\psi}_1^\dagger\hat{\psi}_2^\dagger\hat{\psi}_2\hat{\psi}_1$ and spin-flip couplings of $|m_1\rangle+|m_2\rangle \leftrightarrow |m_1+1\rangle+|m_2-1\rangle$ (with $(m_1,m_2)=\{(1,1),(0,0),(-1,-1),(1,-1),(0,-1),(1,0)\}$) [2]. The Floquet engineering of the quadratic Zeeman energy manipulates all these spin-flip couplings by modulating their relative strengths via Bessel functions. Take the spin-flip process $\hat{\psi}_{-1}^\dagger\hat{\psi}_0^\dagger\hat{\psi}_1\hat{\psi}_{-2}$ as an example:

$$\begin{aligned}&\hat{\psi}_{-1}^\dagger\hat{\psi}_0^\dagger\hat{\psi}_1\hat{\psi}_{-2}\\ &\to\int dt e^{-i4\mathcal{Q}\sin(\omega t)}\hat{\phi}_{-1}^\dagger\hat{\phi}_0^\dagger\hat{\phi}_1\hat{\phi}_{-2}=J_0(4\mathcal{Q})\hat{\phi}_{-1}^\dagger\hat{\phi}_0^\dagger\hat{\phi}_1\hat{\phi}_{-2}\\ &=\hat{\phi}_{-1}^\dagger\hat{\phi}_0^\dagger\hat{\phi}_1\hat{\phi}_{-2}+\left[J_0(4\mathcal{Q})-1\right]\hat{\phi}_{-1}^\dagger\hat{\phi}_0^\dagger\hat{\phi}_1\hat{\phi}_{-2}.\end{aligned} \tag{8}$$

Therefore, it seems that the Floquet engineering gives the Bessel function $J_0(4\mathcal{Q})$ modulation of the strength to this process. The engineering does not modify density couplings since there is no time-dependent phase involved after the transformation. Take the density coupling $\hat{\psi}_1^\dagger\hat{\psi}_2^\dagger\hat{\psi}_2\hat{\psi}_1$ as an example:

$$\hat{\psi}_1^\dagger\hat{\psi}_2^\dagger\hat{\psi}_2\hat{\psi}_1\to\int dt\hat{\phi}_1^\dagger\hat{\phi}_2^\dagger\hat{\phi}_2\hat{\phi}_1=\hat{\phi}_1^\dagger\hat{\phi}_2^\dagger\hat{\phi}_2\hat{\phi}_1. \tag{9}$$

All these density couplings together with spin-flip couplings as the first term in the last equation in Eq. (8) are re-expressed as $(\hat{\phi}^\dagger\mathbf{F}\hat{\phi})\cdot(\hat{\phi}^\dagger\mathbf{F}\hat{\phi})$ which appears in Eq. (6). The Bessel-function modulated spin-flip results, like the term with coefficient $J_0(4\mathcal{Q})-1$ in the last equation in Eq. (8), are assembled into a group leaded by coefficient c_1 in $\hat{H}_{\text{sf}}$. In the same way, the Floquet engineering of the quadratic Zeeman energy also modulates the spin-flip processes in the spin-singlet channel which are $2|0\rangle \leftrightarrow |1\rangle+|-1\rangle$, $2|0\rangle \leftrightarrow |2\rangle+|-2\rangle$, and $|1\rangle+|-1\rangle \leftrightarrow |2\rangle+|-2\rangle$. They are assembled into the other group leaded by c_2 in $\hat{H}_{\text{sf}}$. The minus signs in the front of coupling strengths in some terms originate from a minus sign in the field operator of the spin-singlet pair $\hat{\psi}^T A\hat{\psi}=2\hat{\psi}_2\hat{\psi}_{-2}-2\hat{\psi}_1\hat{\psi}_{-1}+\hat{\psi}_0\hat{\psi}_0$.

Floquet engineering of the quadratic Zeeman energy provides an experimentally accessible method for tuning the interactions in a spin-2 spinor BEC. This is possible because the quadratic Zeeman shift does not commute with the interactions in the Hamiltonian. We derive the similar Floquet-engineered effective Hamiltonian, $\hat{H}_{\text{eff}}$ in Eq. (6) using the high-frequency expansion method [38, 41]; detailed calculations are provided in the appendix. The derivation clearly shows that this non-commutation leads to the non-trivial modulation of interactions. It is well-known that the interactions in spin-2 spinor BECs possess SO(3) symmetry in spin space. Consequently, any unitary transformation generated by the spin operators, such as $\exp(iF_z)$ or $\exp(iF_x)$, leaves the interaction Hamiltonian invariant. This explains why Floquet engineering of typical experimental parameters like the linear Zeeman energy ($\sim F_z$) or a Rabi coupling ($\sim F_x$) cannot tune the interactions, in contrast to the quadratic Zeeman energy.

III. POSSIBLE GROUND STATES

The ground state of a uniform spin-2 spinor BEC can be the polar, ferromagnetic and cyclic phases [2, 21–23]. Due to the Bessel-function modulations of all spin-flip interacting couplings introduced by Floquet engineering, it is crucial to investigate how the ground-state phases and the overall phase diagram are modified in a spin-2 Floquet spinor BEC.

Possible ground-state phases are analyzed using the mean-field theory. The mean-field approximation replaces field operators by their averaged values, $\hat{\phi}\to\langle\hat{\phi}\rangle=\phi$, which become spinor wavefunctions. Since the system is homogeneous, they are assumed to be $\phi = \sqrt{n}\zeta$, where $n = N/V$ is the density with N the total atom number and V the size of the system and $|\zeta\rangle = (\zeta_2, \zeta_1, \zeta_0, \zeta_{-1}, \zeta_{-2})^T$ is the normalized spinor with $\langle\zeta|\zeta\rangle = 1$. Under the mean-field approximation, the energy functional associated with the effective Hamiltonian in Eq. (6) becomes,

$$\frac{E}{N} = q_0\langle F_z^2\rangle + \frac{\tilde{c}_0}{2} + \frac{\tilde{c}_1}{2}\langle \mathbf{F}\rangle^2 + \frac{\tilde{c}_2}{2}|\Theta|^2 + E_F, \quad (10)$$

with the Floquet engineered nonlinearity

$$\begin{aligned} E_F = \frac{\tilde{c}_1}{2}\Big\{&[J_0(2\mathcal{Q}) - 1]\left(6\zeta_0^*\zeta_0^*\zeta_1\zeta_{-1} + 2\sqrt{6}\zeta_1^*\zeta_1^*\zeta_2\zeta_0\right. \\ &\left.+ 2\sqrt{6}\zeta_{-1}^*\zeta_{-1}^*\zeta_0\zeta_{-2}\right) + 4[J_0(6\mathcal{Q}) - 1]\zeta_{-1}^*\zeta_1^*\zeta_2\zeta_{-2} \\ &+ 2\sqrt{6}[J_0(4\mathcal{Q}) - 1]\left(\zeta_{-1}^*\zeta_0^*\zeta_1\zeta_{-2} + \zeta_0^*\zeta_1^*\zeta_2\zeta_{-1}\right) + \mathbf{c.c.}\Big\} \\ &+ \frac{\tilde{c}_2}{2}\Big\{2[J_0(8\mathcal{Q}) - 1]\zeta_0^*\zeta_0^*\zeta_2\zeta_{-2} - 4[J_0(6\mathcal{Q}) - 1] \\ &\times \zeta_{-1}^*\zeta_1^*\zeta_2\zeta_{-2} - 2[J_0(2\mathcal{Q}) - 1]\zeta_0^*\zeta_0^*\zeta_1\zeta_{-1} + \mathbf{c.c.}\Big\}. \quad (11) \end{aligned}$$

The interacting coefficients are rescaled as $\tilde{c}_0 = c_0N$, $\tilde{c}_1 = c_1N$ and $\tilde{c}_2 = c_2N$. In Eq. (10), there are three order parameters, $\langle F_z^2\rangle = \langle\zeta|F_z^2|\zeta\rangle$, $\langle\mathbf{F}\rangle = \langle\zeta|\mathbf{F}|\zeta\rangle$, and $\Theta = (|\zeta\rangle)^T A|\zeta\rangle = 2\zeta_2\zeta_{-2} - 2\zeta_1\zeta_{-1} + \zeta_0^2$. The magnetization of ground states must be aligned with the external magnetic field [2, 21], implying $\langle\mathbf{F}_+\rangle = 0$, where $\mathbf{F}_+ = F_x + iF_y$, i.e., there is no transverse magnetization. Therefore, we have

$$\langle\mathbf{F}\rangle = \langle F_z\rangle, \quad (12)$$

for ground states. Moreover, due to $e^{i\theta F_z}\hat{H}_{\rm eff}e^{-i\theta F_z} = \hat{H}_{\rm eff}$ with θ being an arbitrary angle, the longitudinal magnetization $\langle F_z\rangle$ is conserved, and we set its value as $\langle F_z\rangle = 0$. Under this condition, we have $\tilde{c}_1\langle\mathbf{F}\rangle^2 = 0$, indicating that the spin-dependent interaction $\tilde{c}_1\langle\mathbf{F}\rangle^2$ does not have a contribution to ground state. But the Bessel-function modulated interaction with the coefficient $\tilde{c}_1$ in E_F shall affect on possible ground state. Therefore, the constraint $\langle F_z\rangle = 0$ can emphasis the role of Floquet engineered interactions. The spin configuration of the spinor $|\zeta\rangle$ is determined by minimizing the energy functional under several constraints, such as, the normalization condition, the conservation of $\langle F_z\rangle$, and no transverse magnetization [42]. They are respectively listed as follows,

$$\langle\zeta|\zeta\rangle = |\zeta_2|^2 + |\zeta_1|^2 + |\zeta_0|^2 + |\zeta_{-1}|^2 + |\zeta_{-2}|^2 = 1, \quad (13)$$

$$\langle F_z\rangle = 2|\zeta_2|^2 - 2|\zeta_{-2}|^2 + |\zeta_1|^2 - |\zeta_{-1}|^2 = 0, \quad (14)$$

$$\langle\mathbf{F}_+\rangle = 2\zeta_2^*\zeta_1 + \sqrt{6}\zeta_1^*\zeta_0 + \sqrt{6}\zeta_0^*\zeta_{-1} + 2\zeta_{-1}^*\zeta_{-2} = 0. \quad (15)$$

According to results of the minimization with the constraints, possible ground states are identified as polar, ferromagnetic and cyclic phases in the following.

A. Polar phase

The polar phase features a nonzero order parameter of Θ, i.e., $\Theta \neq 0$ [21]. By checking $\Theta = 2\zeta_2\zeta_{-2} - 2\zeta_1\zeta_{-1} + \zeta_0^2$, there are six possible cases to make $\Theta \neq 0$: (1) $\zeta_0 \neq 0$; (2) $\zeta_1 \neq 0$ and $\zeta_{-1} \neq 0$; (3) $\zeta_2 \neq 0$ and $\zeta_{-2} \neq 0$; (4) $\zeta_2 \neq 0$, $\zeta_{-2} \neq 0$, and $\zeta_0 \neq 0$; (5) $\zeta_1 \neq 0$, $\zeta_{-1} \neq 0$, and $\zeta_0 \neq 0$; (6) all $\zeta_i \neq 0$. According to these different cases, we build up trial wavefunctions that satisfy the constraints [2, 23]. After substituting trial wavefunctions into Eq. (10), we get the energy functional. Variational parameters in trial wavefunctions are then determined by minimizing the energy functional.

(1) When $\zeta_0 \neq 0$ and $\zeta_2 = \zeta_{-2} = \zeta_1 = \zeta_{-1} = 0$, we have the polar solution as

$$\mathbf{P_0}: \ \left(\ 0,\ 0,\ e^{i\theta_0},\ 0,\ 0\ \right)^T. \quad (16)$$

Here θ_0 is the U(1) gauge-invariant phase. Its energy is $E_{P_0}/N = \tilde{c}_0/2 + \tilde{c}_2/2$.

(2) When $\zeta_1 \neq 0$ and $\zeta_{-1} \neq 0$, and $\zeta_2 = \zeta_{-2} = \zeta_0 = 0$, the polar solution becomes

$$\mathbf{P_1}: \ \left(\ 0,\ \sqrt{\tfrac{1}{2}}e^{i\theta_1},\ 0,\ \sqrt{\tfrac{1}{2}}e^{i\theta_{-1}},\ 0\ \right)^T, \quad (17)$$

with θ_1 and θ_{-1} being arbitrary angles. Its energy is $E_{P_1}/N = q_0 + \tilde{c}_0/2 + \tilde{c}_2/2$.

(3) When $\zeta_2 \neq 0$ and $\zeta_{-2} \neq 0$, and $\zeta_1 = \zeta_{-1} = \zeta_0 = 0$, the state is

$$\mathbf{P_2}: \ \left(\ \tfrac{\sqrt{2}}{2}e^{i\theta_2},\ 0,\ 0,\ 0,\ \tfrac{\sqrt{2}}{2}e^{i\theta_{-2}}\ \right)^T. \quad (18)$$

Again θ_2 and θ_{-2} are arbitrary angles. Its energy becomes $E_{P_2}/N = 4q_0 + \tilde{c}_0/2 + \tilde{c}_2/2$.

(4) When $\zeta_2 \neq 0$, $\zeta_{-2} \neq 0$ and $\zeta_0 \neq 0$, and $\zeta_1 = \zeta_{-1} = 0$, we find several solutions.

$$\mathbf{P_3}: \ \left(\ \sqrt{\tfrac{1-\beta^2}{2}}e^{i\chi},\ 0,\ \beta,\ 0,\ \sqrt{\tfrac{1-\beta^2}{2}}e^{-i\chi}\ \right)^T, \quad (19)$$

with χ being an arbitrary angle, and

$$\beta = \sqrt{\frac{4q_0 + \tilde{c}_2 - \tilde{c}_2J_0(8\mathcal{Q})}{2\tilde{c}_2 - 2\tilde{c}_2J_0(8\mathcal{Q})}}, \quad (20)$$

and the corresponding energy

$$\frac{E_{P_3}}{N} = 2q_0 + \frac{\tilde{c}_0}{2} + \frac{\tilde{c}_2}{4} + \frac{\tilde{c}_2}{4}J_0(8\mathcal{Q}) - \frac{4q_0^2}{\tilde{c}_2 - \tilde{c}_2J_0(8\mathcal{Q})}. \quad (21)$$

$$\mathbf{P_4}: \ \left(\ -\sqrt{\tfrac{1-\gamma^2}{2}}e^{i\chi},\ 0,\ \gamma,\ 0,\ \sqrt{\tfrac{1-\gamma^2}{2}}e^{-i\chi}\ \right)^T, \quad (22)$$

with

$$\gamma = \sqrt{\frac{4q_0 + \tilde{c}_2 + \tilde{c}_2J_0(8\mathcal{Q})}{2\tilde{c}_2 + 2\tilde{c}_2J_0(8\mathcal{Q})}}, \quad (23)$$

and associated energy

$$\frac{E_{P_4}}{N} = 2q_0 + \frac{\tilde{c}_0}{2} + \frac{\tilde{c}_2}{4} - \frac{\tilde{c}_2}{4} J_0(8\mathcal{Q}) - \frac{4q_0^2}{\tilde{c}_2 + \tilde{c}_2 J_0(8\mathcal{Q})}. \quad (24)$$

$$\mathbf{P_5}: \begin{pmatrix} \frac{\sqrt{1-\beta^2}-\sqrt{1-\gamma^2}}{\sqrt{2}} e^{i\chi} \\ 0 \\ \sqrt{\beta^2+\gamma^2-1} \\ 0 \\ \frac{\sqrt{1-\beta^2}+\sqrt{1-\gamma^2}}{\sqrt{2}} e^{-i\chi} \end{pmatrix}, \quad (25)$$

and its energy is

$$\begin{aligned} \frac{E_{P_5}}{N} =& 4q_0(2-\beta^2-\gamma^2) + \frac{\tilde{c}_0}{2} + 8\tilde{c}_1(1-\beta^2)(1-\gamma^2) \\ &+ \tilde{c}_2[(\beta^4+\gamma^4)-(\beta^2+\gamma^2)] \\ &+ \tilde{c}_2 J_0(8\mathcal{Q})[(\gamma^4-\beta^4)-(\gamma^2-\beta^2)]. \end{aligned} \quad (26)$$

Note that in the solutions of $\mathbf{P_3}$, $\mathbf{P_4}$ and $\mathbf{P_5}$ the nonlinear coefficient $\tilde{c}_2$ not only affect on the energy but also participates to wavefunctions. While there is no $\tilde{c}_1$ in the wavefunctions, as in the Floquet engineered nonlinear E_F in Eq. (11) the working of $\tilde{c}_1$ requires $\zeta_1 \neq 0$ or $\zeta_{-1} \neq 0$.

(5) In the case of $\zeta_2 = \zeta_{-2} = 0$, $\zeta_1 \neq 0$, $\zeta_0 \neq 0$, and $\zeta_{-1} \neq 0$, we find polar solution

$$\mathbf{P_6}: \left(0,\ -\sqrt{\tfrac{1-\alpha^2}{2}} e^{i\chi},\ \alpha,\ \sqrt{\tfrac{1-\alpha^2}{2}} e^{-i\chi},\ 0 \right)^T. \quad (27)$$

with

$$\alpha = \sqrt{\frac{1}{2} - \frac{q_0}{2(3\tilde{c}_1 - \tilde{c}_2)[1-J_0(2\mathcal{Q})]}}, \quad (28)$$

and its energy is

$$\begin{aligned} \frac{E_{P_6}}{N} =& \frac{q_0}{2} + \frac{\tilde{c}_0}{2} + \frac{\tilde{c}_2}{2} + \frac{q_0^2}{4(3\tilde{c}_1-\tilde{c}_2)[1-J_0(2\mathcal{Q})]} \\ &+ \frac{(3\tilde{c}_1-\tilde{c}_2)[1-J_0(2\mathcal{Q})]}{4}. \end{aligned} \quad (29)$$

It has already been shown that this solution cannot exist in a conventional spin-2 condensate [2]. Our result is consistent with this conclusion: When $\mathcal{Q} = 0$, $J_0(2\mathcal{Q}) = 1$, which leads to the non-definition of α from Eq. (28) if $q_0 \neq 0$. The interesting finding is that the driving can support its existence, which becomes a unique feature of Floquet spinor BECs.

Finally, we comment on the case of (6) that all $\zeta_i \neq 0$. In order to have the zero transverse magnetization, the solution in the case (6) should be the superposition of the solution of $\mathbf{P_2}$ and $\mathbf{P_6}$. However, since $\mathbf{P_2}$ and $\mathbf{P_6}$ have different chemical potential, the superposition cannot lead to a stationary ground state.

B. Ferromagnetic phase

The ferromagnetic phase belongs to eigenstates of F_z. There are the following possible states:

$$\mathbf{F_1}: \left(0,\ e^{i\theta_1},\ 0,\ 0,\ 0 \right)^T, \quad (30)$$

with the energy $E_{F_1}/N = q_0 + \tilde{c}_0/2 + \tilde{c}_1/2$, and

$$\mathbf{F_2}: \left(e^{i\theta_2},\ 0,\ 0,\ 0,\ 0 \right)^T, \quad (31)$$

with the energy $E_{F_2}/N = 4q_0 + \tilde{c}_0/2 + 2\tilde{c}_1$.

C. Cyclic phase

The cyclic phase features $\Theta = 0$ [21–23]. We use the same approach for the previous study of polar phases to construct cyclic wavefunctions considering a more constraint $\Theta = 2\zeta_2\zeta_{-2} - 2\zeta_1\zeta_{-1} + \zeta_0^2 = 0$. The possible solutions are:

$$\mathbf{C_1}: \left(\sqrt{\tfrac{1}{3}} e^{i\theta_2},\ 0,\ 0,\ \sqrt{\tfrac{2}{3}} e^{i\theta_{-1}},\ 0 \right)^T, \quad (32)$$

with the energy $E_{C_1}/N = 2q_0 + \tilde{c}_0/2$, and

$$\mathbf{C_2}: \left(0,\ \sqrt{\tfrac{2}{3}} e^{i\theta_1},\ 0,\ 0,\ \sqrt{\tfrac{1}{3}} e^{i\theta_{-2}} \right)^T, \quad (33)$$

with the energy $E_{C_2}/N = 2q_0 + \tilde{c}_0/2$, and

$$\mathbf{C_3}: \left(\tfrac{1}{2} e^{i\chi},\ 0,\ \tfrac{\sqrt{2}}{2},\ 0,\ -\tfrac{1}{2} e^{-i\chi} \right)^T, \quad (34)$$

with the energy

$$\frac{E_{C_3}}{N} = 2q_0 + \frac{\tilde{c}_0}{2} + \frac{\tilde{c}_2 - \tilde{c}_2 J_0(8\mathcal{Q})}{4}. \quad (35)$$

Note that the spin structure of $\mathbf{C_3}$ is similar to that of polar phases $\mathbf{P_3}$, $\mathbf{P_4}$, and $\mathbf{P_5}$. However, for the cyclic state $\mathbf{C_3}$, the interaction coefficient $\tilde{c}_2$ does not enter into the wavefunction but changes the energy of the state.

IV. PHASE DIAGRAMS

Once possible ground states are known, it would be interesting to show how they participate to phase diagram in the parameter space of periodic driving $(q_0, \mathcal{Q})$. As the spin-singlet scattering $\tilde{c}_2$ may play an important role in above ground states, we consider different phase diagrams by varying the sign of $\tilde{c}_2$ for the fixed spin-independent interaction $\tilde{c}_0 > 0$ and spin-spin interaction $\tilde{c}_1 > 0$.

Fig. 1 demonstrates a ground-state phase diagram for a positive $\tilde{c}_2$. Features of this phase diagram are addressed as follows.

(i) As shown in Fig. 1(a), in the absence of the modulation, $\mathcal{Q} = 0$, ground state is in the polar phase. When

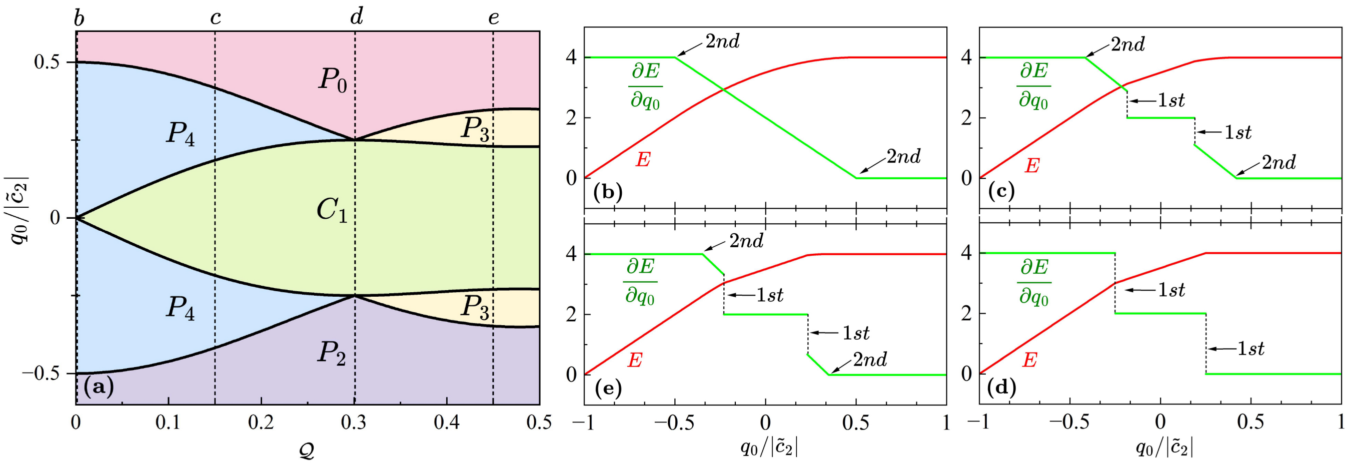

FIG. 1. Phase diagram for a positive $\tilde{c}_2 > 0$. (a) Diagram in the parameter space of periodic driving $(q_0, \mathcal{Q} = Q/(\hbar\omega))$. Vertical dashed lines labeled by b,c,d,e correspond to $\mathcal{Q} = (0, 0.15, 0.3006, 0.45)$ respectively. The energy E (red lines) and derivative of energy $\partial E/\partial q_0$ (green lines) along these labeled lines are demonstrated in (b) ($\mathcal{Q} = 0$), (c) ($\mathcal{Q} = 0.15$), (d) ($\mathcal{Q} = 0.3006$) and (e) ($\mathcal{Q} = 0.45$), respectively. The unit of energy is $|\tilde{c}_2|$. Other parameters are $\tilde{c}_0 = 7\,|\tilde{c}_2|$ and $\tilde{c}_1 = 0.5\,|\tilde{c}_2|$.

$|q_0|$ becomes large, the polar phase belongs to eigenstates of F_z^2. In order to minimize the energy of $q_0\langle F_z^2\rangle$, when $q_0 > \tilde{c}_2/2$ ground state is $\mathbf{P_0}$ which is the eigenstate of F_z^2 with the eigenvalue 0; when $q_0 < -\tilde{c}_2/2$ ground state is $\mathbf{P_2}$ which is the eigenstate of F_z^2 with the eigenvalue 4. For the polar state $\mathbf{P_4}$, $\gamma = \sqrt{(2q_0 + \tilde{c}_0)/2\tilde{c}_2}$ and $\sqrt{(1-\gamma^2)/2} = \sqrt{(\tilde{c}_2 - 2q_0)/4\tilde{c}_2}$, the existence of which requires $-\tilde{c}_2/2 < q_0 < \tilde{c}_2/2$. Since the energy of $\mathbf{P_4}$ is always lower than $\mathbf{P_0}$ and $\mathbf{P_2}$, $\mathbf{P_4}$ becomes ground state in the region of $-\tilde{c}_2/2 < q_0 < \tilde{c}_2/2$. Fig. 1(b) describes the evolution of the energy as a function of q_0. From the derivative curve (the green line), we identify the existence of the second-order phase transitions between $\mathbf{P_2}$ and $\mathbf{P_4}$ at $q = -\tilde{c}_2/2$ and between $\mathbf{P_4}$ and $\mathbf{P_0}$ at $q = \tilde{c}_2/2$.

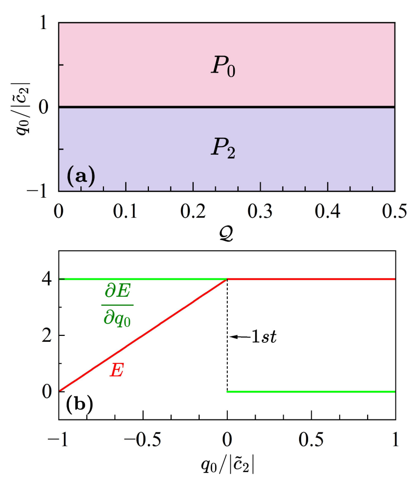

FIG. 2. Phase diagram for the positive $\tilde{c}_2 < 0$. (a) Diagram in the parameter space of periodic driving $(q_0, \mathcal{Q} = Q/(\hbar\omega))$. (b) Evolutions of the energy and the derivative of energy as a function of q_0 at $\mathcal{Q} = 0.2$. Other parameters are the same as Fig. 1.

(ii) In Fig. 1(a), as increasing $\mathcal{Q}$ from 0, a new ground state of cyclic phase $\mathbf{C_1}$ appears locating around the center of $\mathbf{P_4}$ region and therefore splits the $\mathbf{P_4}$ region into two areas. The energy difference $E_{P_4} - E_{C_1} = \tilde{c}_2(1 - J_0(8\mathcal{Q})/4 - 4q_0^2/(\tilde{c}_2(1 + J_0(8\mathcal{Q})))$. In the region of $-\tilde{c}_2\sqrt{1 - J_0(8\mathcal{Q})}/4 < q_0 < \tilde{c}_2\sqrt{1 - J_0(8\mathcal{Q})}/4$, $E_{P_4} - E_{C_1} > 0$, indicating that $\mathbf{C_1}$ is the preferable ground state. The boundaries of $\mathbf{C_1}$ lie at $q_0 = \pm\tilde{c}_2\sqrt{1 - J_0(8\mathcal{Q})}/4$ and consequently extend with the crease of $\mathcal{Q}$. Meanwhile, the existence of $\mathbf{P_4}$ requires $-\tilde{c}_2(1 + J_0(8\mathcal{Q}))/4 < q_0 < \tilde{c}_2(1 + J_0(8\mathcal{Q}))/4$. Its boundaries $q_0 = \pm\tilde{c}_2(1 + J_0(8\mathcal{Q}))/4$ shrink with the increase of $\mathcal{Q}$. The extension and shrink of these two kinds of boundaries finally lead to the $\mathbf{P_4}$ regions shrink into two points at $\mathcal{Q} = 0.3006$. The physical reason for the disappearance of the $\mathbf{P_4}$ phase is that at $\mathcal{Q} = 0.3006$, $J_0(8\mathcal{Q}) = 0$ leads to the boundaries of $\mathbf{C_1}$ and $\mathbf{P_4}$ phases becoming equal.

The evolutions of the energy as a function of q_0 at $\mathcal{Q} = 0.15$ and $\mathcal{Q} = 0.3006$ are demonstrated in Figs. 1(c) and 1(d) respectively. The calculation of the derivative of energy (green lines) indicates that both the transitions between $\mathbf{C_1}$ and $\mathbf{P_4}$ and the transitions between $\mathbf{C_1}$ and $\mathbf{P_0}$ are first order.

(iii) As further increasing $\mathcal{Q}$ from $\mathcal{Q} = 0.3006$, the other new polar phase $\mathbf{P_3}$ appears at the edges of $\mathbf{C_1}$ region [see Fig. 1(a)]. Physically, $\mathbf{P_3}$ state is closely similar to $\mathbf{P_4}$ but with the opposite sign in the front of $J_0(8\mathcal{Q})$. When $\mathcal{Q} > 0.3006$, $J_0(8\mathcal{Q}) < 0$. It seems that $\mathbf{P_3}$ state takes over the region of $\mathbf{P_4}$ due to negative values of $J_0(8\mathcal{Q})$. The derivative of energy as a function of q_0 shown in Fig. 1(e) illustrates that the transitions between $\mathbf{C_1}$ and $\mathbf{P_3}$ are first order and the transitions between $\mathbf{P_3}$ and $\mathbf{P_0}$ and between $\mathbf{P_3}$ and $\mathbf{P_2}$ are second order, providing a further information of the similarity of $\mathbf{P_3}$ and

$\mathbf{P_4}$ phases.

Figure 2 presents a phase diagram for parameter identical to those in Fig. 1, but with $\tilde{c}_2 < 0$. In contrast to the previous case, this diagram is remarkably simple, comprising only the $\mathbf{P_0}$ and $\mathbf{P_2}$ phases [see Fig. 2(a)]. Furthermore, the driving has no effect on the phase boundaries, indicating that the Floquet and conventional spinor BECs are identical for this parameter set. The energy diagram in Fig. 2(b) confirms that the transition between these phases is first order.

V. CONCLUSIONS

We propose to implement a spin-2 Floquet spinor BEC by Floquet engineering of the quadratic Zeeman energy. Coupling strengths of all spin-flip interacting processes that conserve angular momentum in spin-2 Floquet spinor BECs are effectively modulated by Bessel functions which depend on driving parameters. By changing driving parameters, interaction coefficients of all these processes can be relatively tuned. Considering experimental accessibility to adjust the quadratic Zeeman energy, the proposed Floquet system provides a significant platform with tunable spin-dependent interactions. As shown in Ref. [37] in a spin-1 spinor BEC, the spin-flip interacting coupling has an important effect on the spin-mixing dynamics, spin-2 Floquet spinor BECs are another ideal systems to explore spin dynamics.

We find that the Floquet-engineered interactions can significantly influence possible ground states in a homogeneous system. In particular, they support novel ground states that are absent in conventional spin-2 spinor condensates. Ground-state phase diagrams are analyzed for fixed interaction coefficients, illustrating the distribution of possible ground states in the space of driving parameters.

VI. ACKNOWLEDGMENTS

This work is supported by the National Natural Science Foundation of China (NSFC) under Grants No. 12374247 and No. 11974235, as well as by the Shanghai Municipal Science and Technology Major Project (Grant No. 2019SHZDZX01-ZX04).

VII. APPENDIX

We derive the similar Floquet engineered Hamiltonian $\hat{H}_{\text{eff}}$ in Eq. (6) using the high-frequency expansion [41]. This approach emphasizes the importance of non-communication between the quadratic Zeeman energy and the interactions.

To proceed, we first rewrite the Hamiltonian in Eq. (1) as [41]

$$\hat{H} = \hat{H}_0 + \hat{V}\cos(\omega t), \tag{36}$$

with

$$\begin{aligned}\hat{H}_0 = &\int d\mathbf{r}\hat{\psi}^\dagger\left(-\frac{\hbar^2\nabla^2}{2M}\right)\hat{\psi} + \int d\mathbf{r}\hat{\psi}^\dagger\left(q_0F_z^2\right)\hat{\psi}\\ &+\frac{c_0}{2}\int d\mathbf{r}\left(\hat{\psi}^\dagger\hat{\psi}\right)^2 + \frac{c_1}{2}\int d\mathbf{r}\left(\hat{\psi}^\dagger\mathbf{F}\hat{\psi}\right)\cdot\left(\hat{\psi}^\dagger\mathbf{F}\hat{\psi}\right)\\ &+\frac{c_2}{2}\int d\mathbf{r}\left(\hat{\psi}^T A\hat{\psi}\right)^\dagger\left(\hat{\psi}^T A\hat{\psi}\right),\end{aligned}$$

and

$$\hat{V} = \int d\mathbf{r}\hat{\psi}^\dagger\left(QF_z^2\right)\hat{\psi}.$$

The evolution operator is $U(T,0) = \mathcal{T}\exp(-i/\hbar\int_0^T dt\hat{H})$ with $T = 2\pi/\omega$ and $\mathcal{T}$ denoting the time-ordering. The Floquet Hamiltonian $\hat{H}_{\text{eff}}$ is defined as [40]

$$\mathcal{T}e^{-i/\hbar\int_0^T dt\hat{H}} = e^{-i/\hbar\hat{H}_{\text{eff}}T}. \tag{37}$$

Assume ω is high, and Q/ω shall be a small quantity. Using high-frequency expansion, we get [41],

$$\hat{H}_{\text{eff}} = \hat{H}_0 + \frac{1}{4(\hbar\omega)^2}\left[\left[\hat{V},\hat{H}_0\right],\hat{V}\right] + \mathcal{O}(Q^3/\omega^3). \tag{38}$$

The commutator is calculated

$$\begin{aligned}&\left[\left[\hat{V},\hat{H}_0\right],\hat{V}\right]\\ &= -4Q^2c_1\int d\mathbf{r}\Big(3\hat{\psi}_0^\dagger\hat{\psi}_0^\dagger\hat{\psi}_1\hat{\psi}_{-1} + \sqrt{6}\hat{\psi}_1^\dagger\hat{\psi}_1^\dagger\hat{\psi}_2\hat{\psi}_0\\ &+\sqrt{6}\hat{\psi}_{-1}^\dagger\hat{\psi}_{-1}^\dagger\hat{\psi}_0\hat{\psi}_{-2} + 18\hat{\psi}_{-1}^\dagger\hat{\psi}_1^\dagger\hat{\psi}_2\hat{\psi}_{-2}\\ &+4\sqrt{6}\hat{\psi}_{-1}^\dagger\hat{\psi}_0^\dagger\hat{\psi}_1\hat{\psi}_{-2} + 4\sqrt{6}\hat{\psi}_0^\dagger\hat{\psi}_1^\dagger\hat{\psi}_2\hat{\psi}_{-1} + \text{H.c.}\Big)\\ &-4Q^2c_2\int d\mathbf{r}\Big(-\hat{\psi}_0^\dagger\hat{\psi}_0^\dagger\hat{\psi}_1\hat{\psi}_{-1} + 16\hat{\psi}_0^\dagger\hat{\psi}_0^\dagger\hat{\psi}_2\hat{\psi}_{-2}\\ &-18\hat{\psi}_{-1}^\dagger\hat{\psi}_1^\dagger\hat{\psi}_2\hat{\psi}_{-2} + \text{H.c.}\Big),\end{aligned} \tag{39}$$

which is a signature of the non-communication between the quadratic Zeeman energy and the interactions. By substituting the above result into Eq. (38), we obtain the Floquet Hamiltonian,

$$
\begin{aligned}
\hat{H}_{\text{eff}} =& \hat{H}_0 - \frac{c_1}{2}\left(\frac{Q}{\hbar\omega}\right)^2 \int d\mathbf{r} \left(6\hat{\psi}_0^\dagger\hat{\psi}_0^\dagger\hat{\psi}_1\hat{\psi}_{-1} + 2\sqrt{6}\hat{\psi}_1^\dagger\hat{\psi}_1^\dagger\hat{\psi}_2\hat{\psi}_0 + 2\sqrt{6}\hat{\psi}_{-1}^\dagger\hat{\psi}_{-1}^\dagger\hat{\psi}_0\hat{\psi}_{-2} + 36\hat{\psi}_{-1}^\dagger\hat{\psi}_1^\dagger\hat{\psi}_2\hat{\psi}_{-2}\right. \\
& \left. +8\sqrt{6}\hat{\psi}_{-1}^\dagger\hat{\psi}_0^\dagger\hat{\psi}_1\hat{\psi}_{-2} + 8\sqrt{6}\hat{\psi}_0^\dagger\hat{\psi}_1^\dagger\hat{\psi}_2\hat{\psi}_{-1} + \text{H.c.}\right) - \frac{c_2}{2}\left(\frac{Q}{\hbar\omega}\right)^2 \int d\mathbf{r} \left(32\hat{\psi}_0^\dagger\hat{\psi}_0^\dagger\hat{\psi}_2\hat{\psi}_{-2} - 36\hat{\psi}_{-1}^\dagger\hat{\psi}_1^\dagger\hat{\psi}_2\hat{\psi}_{-2}\right. \\
& \left. -2\hat{\psi}_0^\dagger\hat{\psi}_0^\dagger\hat{\psi}_1\hat{\psi}_{-1} + \text{H.c.}\right),
\end{aligned} \tag{40}
$$

Note that there is a difference between the above Hamiltonian from the high-frequency expansion and the engineered one from unitary transformation and time average in Eq. (6), as we only keep the second order of the perturbation of $Q/(\hbar\omega)$ in Eq. (38). By expanding the Bessel function $J_0(jQ/(\hbar\omega)) \approx 1 - j^2Q^2/(4\hbar^2\omega^2)$ with the assumption $jQ/(\hbar\omega)$ being a small quantity, the effective Hamiltonian in Eq. (6) automatically turns to be the perturbed one in Eq. (40).

[1] D. M. Stamper-Kurn and M. Ueda, Spinor Bose gases: Symmetries, magnetism, and quantum dynamics, Rev. Mod. Phys. **85**, 1191 (2013).

[2] Y. Kawaguchi and M. Ueda, Spinor Bose-Einstein condensates, Phys. Rep. **520**, 253 (2012).

[3] Tin-Lun Ho, Spinor Bose Condensates in Optical Traps, Phys. Rev. Lett. **81**, 742 (1998).

[4] T. Ohmi and K. Machida, Bose-Einstein Condensation with Internal Degrees of Freedom in Alkali Atom Gases, J. Phys. Soc. Jpn. **67**, 1822 (1998).

[5] Keiji Murata, Hiroki Saito, and Masahito Ueda, Broken-axisymmetry phase of a spin-1 ferromagnetic Bose-Einstein condensate, Phys. Rev. A **75**, 013607 (2007).

[6] J. Stenger, S. Inouye, D. M. Stamper-Kurn, H.-J. Miesner, A. P. Chikkatur, and W. Ketterle, Spin domains in ground-state Bose–Einstein condensates, Nature (London) **396**, 345 (1998).

[7] M.-S. Chang, C. D. Hamley, M. D. Barrett, J. A. Sauer, K. M. Fortier, W. Zhang, L. You, and M. S. Chapman, Observation of Spinor Dynamics in Optically Trapped 87Rb Bose-Einstein Condensates , Phys. Rev. Lett. **92**, 140403 (2004).

[8] Y. Liu, S. Jung, S. E. Maxwell, L. D. Turner, E. Tiesinga, and P. D. Lett, Quantum Phase Transitions and Continuous Observation of Spinor Dynamics in an Antiferromagnetic Condensate, Phys. Rev. Lett. **102**, 125301 (2009).

[9] F. Gerbier, A. Widera, S. Fölling, O. Mandel, and I. Bloch, Resonant control of spin dynamics in ultracold quantum gases by microwave dressing, Phys. Rev. A **73**, 041602 (2006).

[10] S. R. Leslie, J. Guzman, M. Vengalattore, J. D. Sau, M. L. Cohen, and D. M. Stamper-Kurn, Amplification of fluctuations in a spinor Bose-Einstein condensate, Phys. Rev. A **79**, 043631 (2009).

[11] E. M. Bookjans, A. Vinit, and C. Raman, Quantum Phase Transition in an Antiferromagnetic Spinor Bose-Einstein Condensate, Phys. Rev. Lett. **107**, 195306 (2011).

[12] M. Anquez, B. A. Robbins, H. M Bharath, M. Boguslawski, T. M. Hoang, and M. S. Chapman, Quantum Kibble-Zurek Mechanism in a Spin-1 Bose-Einstein Condensate, Phys. Rev. Lett. **116**, 155301(2016).

[13] H.-X. Yang, T. Tian, Y.-B. Yang, L.-Y. Qiu, H.-Y. Liang, A.-J. Chu, C. B. Dağ, Y. Xu, Y. Liu, and L.-M. Duan, Observation of dynamical quantum phase transitions in a spinor condensate, Phys. Rev. A **100**, 013622 (2019).

[14] Jie Zhang, Z. F. Xu, L. You, and Yunbo Zhang, Atomic-number fluctuations in a mixture of condensates, Phys. Rev. A **82**, 013625 (2010).

[15] Yu Shi, Ground states of a mixture of two species of spinor Bose gases with interspecies spin exchange, Phys. Rev. A **82**, 023603 (2010).

[16] Z. F. Xu, J. W. Mei, R. Lü, and L. You, Spontaneously axisymmetry-breaking phase in a binary mixture of spinor Bose-Einstein condensates, Phys. Rev. A **82**, 053626 (2010).

[17] Xiaoke Li, Bing Zhu, Xiaodong He, Fudong Wang, Mingyang Guo, Zhi-Fang Xu, Shizhong Zhang, and Dajun Wang, Coherent Heteronuclear Spin Dynamics in an Ultracold Spinor Mixture, Phys. Rev. Lett. **114**, 255301 (2015).

[18] A. Görlitz, T. L. Gustavson, A. E. Leanhardt, R. Löw, A. P. Chikkatur, S. Gupta, S. Inouye, D. E. Pritchard, and W. Ketterle, Sodium Bose-Einstein Condensates in the $F = 2$ State in a Large-Volume Optical Trap, Phys. Rev. Lett. **90**, 090401 (2003).

[19] H. Schmaljohann, M. Erhard, J. Kronjäger, M. Kottke, S. van Staa, L. Cacciapuoti, J. J. Arlt, K. Bongs, and K. Sengstock, Dynamics of $F = 2$ Spinor Bose-Einstein Condensates, Phys. Rev. Lett. **92**, 040402 (2004).

[20] C. Klempt, O. Topic, G. Gebreyesus, M. Scherer, T. Henninger, P. Hyllus, W. Ertmer, L. Santos, and J. J. Arlt, Multiresonant Spinor Dynamics in a Bose-Einstein Condensate,Phys. Rev. Lett. **103**, 195302 (2009) .

[21] C. V. Ciobanu, S. K. Yip, and T.-L. Ho, Phase diagrams of F=2 spinor Bose-Einstein condensates, Phys. Rev. A **61**, 033607 (2000).

[22] Masahito Ueda and Masato Koashi, Theory of spin-2 Bose-Einstein condensates: Spin correlations, magnetic response, and excitation spectra, Phys. Rev. A **65**, 063602 (2002).

[23] G. P. Zheng, Y. G. Tong, and F. L. Wang, Ground states of spin-2 condensates in an external magnetic field, Phys. Rev. A **81**, 063633 (2010).

[24] Y. Kawaguchi and M. Ueda, Symmetry classification of spinor Bose-Einstein condensates, Phys. Rev. A **84**, 053616 (2011).

[25] M. Kobayashi and M. Nitta, Symmetry classification of uniform states in spin-2 Bose-Einstein condensates and neutron $^3P_2$ superfluids, Phys. Rev. A **104**, 053302 (2021).

[26] G. C. Katsimiga, S. I. Mistakidis, P. Schmelcher, and P. G. Kevrekidis, Phase diagram, stability and magnetic properties of nonlinear excitations in spinor Bose-Einstein condensates, New J. Phys. **23**, 013015 (2021).

[27] Yu Shi, and Qian Niu, Bose-Einstein Condensation with an Entangled Order Parameter, Phys. Rev. Lett. **96** 140401 (2006).

[28] H. H. Jen and S. K. Yip, Fragmented many-body states of a spin-2 Bose gas, Phys. Rev. A **91** 063603 (2015).

[29] A. M. Turner, R. Barnett, E. Demler, and A. Vishwanath, Nematic order by disorder in spin-2 Bose-Einstein condensates, Phys. Rev. Lett. **98** 190404 (2007).

[30] G. Baio, M. T. Wheeler, D. S. Hall, J. Ruostekoski, and M. O. Borgh, Topological interfaces crossed by defects and textures of continuous and discrete point group symmetries in spin-2 Bose-Einstein condensates, Phys. Rev. Res. **6**, 013046 (2024).

[31] Y. Eto, H. Shibayama, H. Saito, and T. Hirano, Spinor dynamics in a mixture of spin-1 and spin-2 Bose- Einstein condensates, Phys. Rev. A **97**, 021602(R) (2018).

[32] Uyen Ngoc Le, Hieu Binh Le, and Hiroki Saito, Phase separation and metastability in a mixture of spin-1 and spin-2 Bose-Einstein condensates, Phys. Rev. A **110**, 033328 (2024).

[33] A. Widera, F. Gerbier, S. Fölling, T. Gericke, O. Mandel, and I. Bloch, Precision measurement of spin-dependent interaction strengths for spin-1 and spin-2 ^{87}Rb atoms, New J. Phys. **8**, 152 (2006).

[34] W. Zhang, D. L. Zhou, M.-S. Chang, M. S. Chapman, and L. You, Dynamical Instability and Domain Formation in a Spin-1 Bose-Einstein Condensate, Phys. Rev. Lett. **95**, 180403 (2005).

[35] D. Jacob, L. Shao, V. Corre, T. Zibold, L. De Sarlo, E. Mimoun, J. Dalibard, and F. Gerbier, Phase diagram of spin-1 antiferromagnetic Bose-Einstein condensates, Phys. Rev. A **86**, 061601 (2012).

[36] H. K. Pechkis, J. P. Wrubel, A. Schwettmann, P. F. Griffin, R. Barnett, E. Tiesinga, and P. D. Lett, Spinor Dynamics in an Antiferromagnetic Spin-1 Thermal Bose Gas, Phys. Rev. Lett. **111**, 025301 (2013).

[37] Q. Guan, D. Blume, and R. J. Lewis-Swan, Controlling the dynamical phase diagram of a spinor Bose-Einstein condensate using time-dependent potentials, Phys. Rev. A **112**, 023306 (2025).

[38] K. Fujimoto and S. Uchino, Floquet spinor Bose gases, Phys. Rev. Res. **1**, 033132 (2019).

[39] Y. Zhang, Y. Chen, H. Lyu, and Y. Zhang, Quantum phases in spin-orbit-coupled Floquet spinor Bose gases, Phys. Rev. Res. **5**, 023160 (2023).

[40] A. Eckardt, Colloquium: Atomic quantum gases in periodically driven optical lattices, Rev. Mod. Phys. **89**, 011004 (2017).

[41] N. Goldman and J. Dalibard, Periodically driven quantum systums: Effective hamiltonians and engineered gauge fields, Phys. Rev. X **4**, 031027 (2014).

[42] W. Zhang, S. Yi, and L. You, Mean field ground state of a spin-1 condensate in a magnetic field, New J. Phys. **5**, 77 (2003).